# Thermal analysis for laser selective removal of metallic single-walled carbon nanotubes

Jizhou Song, Yuhang Li, Frank Du, Xu Xie, Yonggang Huang, and John A. Rogers

**Articles you may be interested in**

Electrical and thermal transport in metallic single-wall carbon nanotubes on insulating substrates
J. Appl. Phys. **101**, 093710 (2007); 10.1063/1.2717855

Stability of ion implanted single-walled carbon nanotubes: Thermogravimetric and Raman analysis
J. Appl. Phys. **100**, 064315 (2006); 10.1063/1.2353643

Reaction Of Single-Wall Carbon Nanotubes With Radicals
AIP Conf. Proc. **723**, 209 (2004); 10.1063/1.1812075

Chirality selection of single-walled carbon nanotubes by laser resonance chirality selection method
Appl. Phys. Lett. **85**, 858 (2004); 10.1063/1.1778471

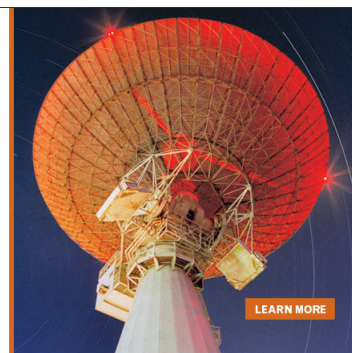Large diameter single-wall carbon nanotubes obtained by pulsed laser vaporization
AIP Conf. Proc. **591**, 191 (2001); 10.1063/1.1426851

# Thermal analysis for laser selective removal of metallic single-walled carbon nanotubes

Jizhou Song,[1,a)] Yuhang Li,[2] Frank Du,[3] Xu Xie,[3] Yonggang Huang,[4] and John A. Rogers[3]

[1]*Department of Engineering Mechanics and Soft Matter Research Center, Zhejiang University, Hangzhou 310027, China*
[2]*The Solid Mechanics Research Center, Beihang University (BUAA), Beijing 100191, China*
[3]*Department of Materials Science and Engineering, Frederick Seitz Materials Research Laboratory, University of Illinois at Urbana-Champaign, Urbana, Illinois 61801, USA*
[4]*Department of Civil and Environmental Engineering, Department of Mechanical Engineering, Center for Engineering and Health, and Skin Disease Research Center, Northwestern University, Evanston, Illinois 60208, USA*

Single-walled carbon nanotubes (SWNTs) have been envisioned as one of the best candidates for future semiconductors due to their excellent electrical properties and ample applications. However, SWNTs grow as mixture of both metallic and semiconducting tubes and this heterogeneity hampers their practical applications. Laser radiation shows promises to remove metallic SWNTs (m-SWNTs) in air under an appropriate condition. We established a scaling law, validated by finite element simulations, for the temperature rise of m-SWNTs under a pulsed laser with a Gaussian spot. It is shown that the maximum normalized m-SWNT temperature rise only depends on two non-dimensional parameters: the normalized pulse duration time and the normalized interfacial thermal resistance. In addition, the maximum temperature rise is inversely proportional to the square of spot size and proportional to the incident laser power. These results are very helpful to understand the underlying physics associated with the removal process and provides easily interpretable guidelines for further optimizations. © 2015 AIP Publishing LLC.
[http://dx.doi.org/10.1063/1.4919591]

## I. INTRODUCTION

Single-walled carbon nanotubes (SWNTs) have been envisioned as one of the most promising candidates for next generation semiconductor materials owing to their superior electrical properties compared to those of silicon.[1–3] However, current synthesis methods lead to the production of mixtures of both metallic and semiconducting tubes, and thus, their practical application to semiconductor electronics is largely hampered.

Horizontally aligned arrays of purely semiconducting SWNTs (s-SWNTs) represent an ideal configuration for applications in electronics because such arrays provide optimal transport pathways from source to drain due to the absence of tube-to-tube junctions.[4–6] SWNT arrays grown using Chemical vapor deposition (CVD) on ST-cut quartz substrates have perfect alignment but contain both metallic SWNTs (m-SWNTs) and s-SWNTs (2/3 are semiconducting and 1/3 are metallic).[7,8] Various approaches have been used to remove m-SWNTs to yield purely s-SWNTs. One approach involves application of large bias voltage to transistors with selective electrical breakdown of m-SWNTs.[9] This process, although successfully employed in circuits,[10] only eliminates certain small segments of the m-SWNTs. Also, the operation must be performed on each individual device. Recently, developed purification techniques based on nanoscale thermocapillary flows in thin films enable complete elimination of m-SWNTs but require multiple

deposition and etching steps to fabricate the necessary transistor or antenna structure and to remove the thin films.[8,11–14]

A scheme bypassing the above drawbacks to yield a simplified, efficient, robust process could be of significant practical value. Figure 1 schematically shows such a scheme using laser radiation to remove m-SWNTs based on the fact that m-SWNTs absorb much more energy and can be destroyed in air in preference to their semiconducting counterparts when wavelength of radiation is appropriate.[15–24] This process begins with the growth of perfectly aligned SWNTs on a quartz substrate as shown in Fig. 1(a). A pulsed
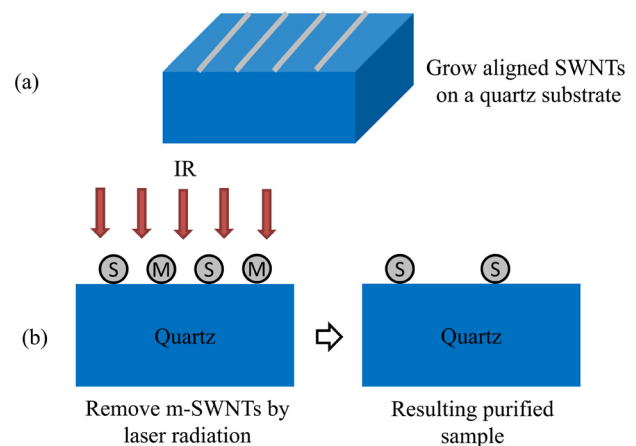


FIG. 1. (a) Schematic diagram of aligned SWNTs on a quartz substrate. (b) Schematic illustration of removing metallic SWNTs by laser radiation.

a)Author to whom correspondence should be addressed. Electronic mail: jzsong@zju.edu.cn.

**117**, 165102-1

infrared laser with a Gaussian spot is then applied to scan the top surface to ablate m-SWNTs and yield arrays of only s-SWNTs as shown in Fig. 1(b). Although the concept of ablation has been demonstrated under some conditions,[15–24] analytical modeling is needed to help the design of experiments to explore further possibilities.

A full understanding of the physics associated with the process of laser-induced selective removal of m-SWNTs is critical to optimize the purification process, i.e., define criteria to select the laser parameters to remove m-SWNTs but leave s-SWNTs. Our objective is to establish an analytical model for selective removal of m-SWNTs under a pulsed laser with a Gaussian spot and to obtain the analytic expression for the SWNT temperature in terms of material properties (e.g., thermal conductivity and thermal diffusivity), geometric (e.g., SWNT radius), and loading parameters (e.g., laser power and pulse duration).

## II. THERMAL MODELING FOR SWNT TEMPERATURE

Thermal modeling provides both qualitative and quantitative insights into the distributions in temperature associated with laser radiation. For simplicity, we ignore the quantum aspects of interactions of laser and carbon nanotubes as well as the thermal processes in carbon nanotubes. This treatment based on classical physics to study the heat flow in carbon nanotubes has been shown by many researchers.[25–27] Figure 2(a) shows a schematic diagram of the analytical model for the case of an individual m-SWNT on a quartz substrate under a pulsed laser with a Gaussian spot. The m-SWNT serves as a surface heat source with the length $2L$ and width $2R$, where $R$ is the radius of m-SWNT, and power density defined by the

laser absorption $q_{total} = \beta I_0$, where $0 < \beta < 1$ is a coefficient depending on the laser wavelength and $I_0$ is the incident power distribution as shown in Fig. 2(b). Although the optical physics of $\beta$ is still not well understood, a simple approximation of $\beta$ can be given by the Beer-Lambert law $\beta = 1 - e^{-\delta d}$, where $\delta$ is the absorption coefficient and $d$ is the distance of the light travels through the material. Here, $d$ can be approximated as twice the wall thickness $h$ of SWNT, i.e., $d \approx 2h$. The origin of the coordinate system $(x, y, z)$ is located at the center of the SWNT with $x$ along the SWNT axis, $y$ along the direction normal to the SWNT axis, and $z$ pointing from the quartz substrate to the top.

A pulsed Gaussian laser source of power $P_0$ yields an incident power distribution $I_0(r) = \frac{P_0}{2\pi\sigma^2} e^{-\frac{r^2}{2\sigma^2}}$ for $0 < t \leq t_d$ and $I_0(r) = 0$ for $t_d < t \leq t_p$ in one period where $r$ is the distance of the point interested to the center of the laser spot, $\sigma$ is the standard deviation, $t_d$ is the pulse duration, and $t_p$ is the pulse period as shown in Fig. 2(b). Since 99% of the energy is confined within the range of $3\sigma$, the radius $S$ of the spot can be approximated by $3\sigma$, i.e., $S = 3\sigma$.

The power density of the m-SWNT ($-L \leq x \leq L$, $-R \leq y \leq R$) is then obtained by $q_{total}(x, y, t) = \frac{(1-e^{-\delta d})P_0}{2\pi\sigma^2} e^{-\frac{x^2}{2\sigma^2}}$ for $0 < t \leq t_d$ and $q_{total}(x, y, t) = 0$ for $t_d < t \leq t_p$. The total energy absorbed by the m-SWNT is used to heat both the substrate and the m-SWNT. Let the heat flux into the substrate $q(x, y, t)$ takes the same form of $q_{total}(x, y, t)$ as $q(x, y, t) = \gamma \cdot q_{total}(x, y, t)$, where $\gamma$ represents the fraction of energy into the substrate and $0 < \gamma < 1$. Then the distribution of the temperature rise $\theta(x, y, z, t) = T(x, y, z, t) - T_\infty$ from the ambient temperature $T_\infty$ in the substrate can be obtained as[28]

$$\theta(x,y,z,t) = \begin{cases} \int_{\tau=0}^{t}\int_{y'=-R}^{R}\int_{x'=-L}^{L} \frac{\gamma \cdot q_{total}(x',y',\tau)}{4\rho c[\pi\alpha(t-\tau)]^{\frac{3}{2}}} e^{-\frac{(x-x')^2+(y-y')^2+z^2}{4\alpha(t-\tau)}} dx'dy'd\tau & 0 < t \leq t_d \\ \int_{\tau=0}^{t_d}\int_{y'=-R}^{R}\int_{x'=-L}^{L} \frac{\gamma \cdot q_{total}(x',y',\tau)}{4\rho c[\pi\alpha(t-\tau)]^{\frac{3}{2}}} e^{-\frac{(x-x')^2+(y-y')^2+z^2}{4\alpha(t-\tau)}} dx'dy'd\tau & \bar{t} < t \leq t_p, \end{cases} \quad (1)$$

where $\rho$ is the substrate density, $\alpha = k/(c\rho)$ is the thermal diffusivity of the substrate with $k$ as the thermal conductivity and $c$ as the specific heat capacity. If the interfacial

thermal resistance between m-SWNT and the substrate is $R_{th}$, the temperature rise of m-SWNT can be approximated by the average temperature rise of heat source plus the
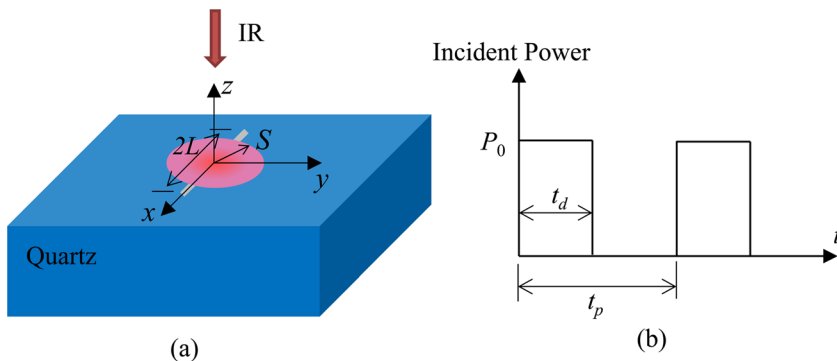


FIG. 2. (a) Schematic diagram of the analytical model. (b) Power of laser with pulse duration time $t_d$ and period $t_p$.

temperature increase due to the interfacial thermal resistance, i.e.,

$$\theta_{SWNT}(x,t) = \begin{cases} \dfrac{1}{2R} \displaystyle\int\limits_{y=-R}^{R} \theta(x,y,z=0,t)dy + qR_{th} & 0 < t \le t_d \\[3mm] \dfrac{1}{2R} \displaystyle\int\limits_{y=-R}^{R} \theta(x,y,z=0,t)dy & t_d < t \le t_p. \end{cases} \tag{2}$$

The energy per unit length into the SWNT is then obtained as $c_{SWNT}\rho_{SWNT}A_{SWNT}\theta_{SWNT}(x,t)$, where $c_{SWNT}$ is the specific heat capacity of SWNT, $\rho_{SWNT}$ is the density of SWNT, and $A_{SWNT} = \pi h(2R - h)$ is the cross-sectional area of SWNT, and $h$ is the wall thickness of SWNT. The total energy per unit length into the system is equal to the energy into the substrate plus the energy into the SWNT. Therefore, we have $q_{total}2Rt = q2Rt + c_{SWNT}\rho_{SWNT}A_{SWNT}\theta_{SWNT}(x,t)$ which gives the fraction of energy $\gamma$ into the substrate.

## III. A SCALING LAW FOR THE MAXIMUM TEMPERATURE RISE

Since the maximum temperature rise determines the condition to remove the m-SWNT, our focus is to establish a scaling law for the maximum temperature rise in terms of material properties, geometric, and loading parameters under short pulsed laser illumination (ns or shorter).

The thermal diffusivity of quartz is $\alpha = 2.7 \times 10^{-6}$ m$^2$/s.[8] The laser spot size $S$ is usually on the order of 10 $\mu$m (Refs. 15, 19, and 22) and therefore $\sigma = S/3$ is on the order of $\mu$m. For the short pulsed laser of ns (or shorter), $\alpha t_d \ll \sigma^2$. Equation (2) then gives the temperature rise of the m-SWNT as

$$\theta_{SWNT}(x,t) = \frac{\gamma(1-e^{-\delta d})P_0}{2\pi\sigma^2}\left[\frac{f(t)}{\pi\rho c\alpha R} + R_{th}\right]e^{-\frac{x^2}{2\sigma^2}}, \tag{3}$$

for $0 \le t \le t_d$, and the fraction of energy into the substrate $\gamma$ is $\gamma = \left[1 + \frac{c_{SWNT}\rho_{SWNT}A_{SWNT}}{2Rt}\left(\frac{f(t)}{\pi\rho c\alpha R} + R_{th}\right)\right]^{-1}$ where $f(t) = 2R\sqrt{\pi\alpha t} \cdot erf\left(\frac{R}{\sqrt{\alpha t}}\right) + \text{Ei}\left(\frac{R^2}{\alpha t}\right)R^2 - \alpha t + \alpha t e^{-\frac{R^2}{\alpha t}}$, $\text{Ei}(x) = \int_1^\infty \frac{e^{-xt}}{t}dt$ is the exponential integral, and $erf(x) = \frac{2}{\sqrt{\pi}}\int_0^x e^{-t^2}dt$. It should be noted that $L$ in Eq. (1) is taken as infinity to obtain Eq. (3) analytically since $L$ is usually much larger than the laser spot size. By introducing the non-dimensional temperature rise $\bar{\theta}_{SWNT} = \frac{\rho c\alpha\sigma^2}{(1-e^{-\delta d})P_0 R}\theta_{SWNT}$, $\bar{x} = x/\sigma$, $\bar{t} = t\alpha/R^2$, $\bar{h} = h/R$, $\bar{\rho}_c = \rho_{SWNT}c_{SWNT}/\rho c$, and $\bar{R}_{th} = R_{th}\rho c\alpha/R$, Eq. (3) becomes

$$\bar{\theta}_{SWNT}(\bar{x}, 0 \le \bar{t} \le \bar{t}_d) = \frac{\gamma}{2\pi^2}\left[\bar{f}(\bar{t}) + \pi\bar{R}_{th}\right]e^{-\frac{\bar{x}^2}{2}}, \tag{4}$$

with $\quad \bar{f}(\bar{t}) = 2\sqrt{\pi\bar{t}} \cdot erf\left(\frac{1}{\sqrt{\bar{t}}}\right) + \text{Ei}\left(\frac{1}{\bar{t}}\right) - \bar{t} + \bar{t}e^{-\frac{1}{\bar{t}}}$ and $\gamma = \left[1 + \frac{\bar{\rho}_c(2-\bar{h})\bar{h}}{2\bar{t}}\left(\bar{f}(\bar{t}) + \pi\bar{R}_{th}\right)\right]^{-1}$. The maximum normalized temperature rise of m-SWNT occurs at $t = t_d$ and

$\bar{x} = 0$, i.e., $\bar{\theta}_{SWNT}^{Max} = \bar{\theta}_{SWNT}(\bar{x} = 0, \bar{t} = t_d)$, therefore, we have

$$\bar{\theta}_{SWNT}^{Max} = \frac{\gamma}{2\pi^2}\left[2\sqrt{\pi\bar{t}_d} \cdot erf\left(\frac{1}{\sqrt{\bar{t}_d}}\right) + \text{Ei}\left(\frac{1}{\bar{t}_d}\right) - \bar{t}_d + \bar{t}_d e^{-\frac{1}{\bar{t}_d}} + \pi\bar{R}_{th}\right], \tag{5}$$

with $\quad \gamma = \left[1 + \frac{\bar{\rho}_c(2-\bar{h})\bar{h}}{2\bar{t}_d}\left(2\sqrt{\pi\bar{t}_d} \cdot erf\left(\frac{1}{\sqrt{\bar{t}_d}}\right) + \text{Ei}\left(\frac{1}{\bar{t}_d}\right) - \bar{t}_d + \bar{t}_d e^{-\frac{1}{\bar{t}_d}} + \pi\bar{R}_{th}\right)\right]^{-1}$, which clearly shows that the maximum normalized temperature rise $\bar{\theta}_{SWNT}^{Max}$ depends on four non-dimensional parameters: the normalized pulse duration time $\bar{t}_d$, the normalized interfacial thermal resistance $\bar{R}_{th}$, the normalized SWNT thickness $\bar{h}$, and the normalized thermal property $\bar{\rho}_c$. Also, the maximum temperature rise is inversely proportional to the square of spot size and proportional to the incident laser power.

For a specific system of m-SWNTs on a quartz substrate, $\bar{\rho}_c = \rho_{SWNT}c_{SWNT}/\rho c = 0.2364$ with $\rho = 2650$ kg m$^{-3}$ and $c = 830$ J kg$^{-1}$ K$^{-1}$ for the quartz,[8] and $\rho_{SWNT} = 1300$ kg m$^{-3}$ and $c_{SWNT} = 400$ J kg$^{-1}$ K$^{-1}$ for SWNTs.[29] The thickness of the m-SWNT is taken as $h = 0.34$nm.[30,31] For simplicity, we fix the SWNT radius to be $R = 1.0$nm in the following to study the effects of laser pulse and interfacial thermal resistance on the m-SWNT temperature. Equation (5) then depends only on the normalized pulse duration time $\bar{t}_d$ and the normalized interfacial thermal resistance $\bar{R}_{th}$, i.e.,

$$\bar{\theta}_{SWNT}^{Max} = \bar{\theta}_{SWNT}^{Max}(\bar{t}_d, \bar{R}_{th}, \bar{h} = 0.34, \bar{\rho}_c = 0.2364). \tag{6}$$

The above scaling law is very helpful to choose appropriate laser pulse to destroy the m-SWNTs.

Equation (6) can be further simplified for two commonly used pulsed lasers with short pulse of $t_d = 10$ns and ultra-short pulse of $t_d = 100$fs. For example, in the case of $t_d = 10$ns, $\bar{t}_d = 2.73 \times 10^4$, $erf\left(\frac{1}{\sqrt{\bar{t}_d}}\right) \approx \frac{2}{\sqrt{\pi\bar{t}_d}}$, $e^{-\frac{1}{\bar{t}_d}} \approx 1 - \frac{1}{\bar{t}_d}$, and $\gamma \approx 1$, which yields the maximum normalized temperature rise as

$$\bar{\theta}_{SWNT}^{Max} = \frac{1}{2\pi^2}\left[3 + \text{Ei}\left(\frac{1}{\bar{t}_d}\right) + \pi\bar{R}_{th}\right]. \tag{7}$$

Equation (7) holds for large $\bar{t}_d$ and the maximum normalized temperature rise depends linearly on the normalized interfacial thermal resistance.

For the case of $t_d = 100$fs, $\bar{t}_d = 0.273$, $erf\left(\frac{1}{\sqrt{\bar{t}_d}}\right) \approx 1$, $e^{-\frac{1}{\bar{t}_d}} \approx 0$, $\text{Ei}\left(\frac{1}{\bar{t}_d}\right) \ll \bar{t}_d$, and $\text{Ei}\left(\frac{1}{\bar{t}_d}\right) \ll \sqrt{\bar{t}_d}$, which yields the maximum normalized temperature rise as

$$\bar{\theta}_{SWNT}^{Max} = \frac{2\sqrt{\pi\bar{t}_d} - \bar{t}_d + \pi\bar{R}_{th}}{2\pi^2\left[1 + \frac{\bar{\rho}_c(2-\bar{h})\bar{h}}{2\bar{t}_d}\left(2\sqrt{\pi\bar{t}_d} - \bar{t}_d + \pi\bar{R}_{th}\right)\right]}. \tag{8}$$

Reported values for the interfacial thermal resistance span a wide range from $10^{-8}$ to $10^{-7}$ m$^2$ K/W,[25,32,33] which gives

$\bar{R}_{th}$ from 60 to 600. Equation (8) can then be further simplified as

$$\bar{\theta}_{SWNT}^{Max} = \frac{\bar{t}_d}{\pi^2 \bar{\rho}_c (2 - \bar{h})\bar{h}}. \tag{9}$$

Equation (9) holds for small $\bar{t}_d$ and the maximum normalized temperature rise becomes independent of the interfacial thermal resistance.

## IV. RESULTS AND DISCUSSION

Figure 3 shows the temperature rise of the m-SWNT versus time with $t_d = 100$fs, $t_p = 1$ms, $P_0 = 1.0$W, $\sigma = 0.6\,\mu m$, $R_{th} = 0$, and $1 - e^{-\delta d} = 0.068$.[24] The thickness and radius of the m-SWNT are taken as $h = 0.34$nm and $R = 1.0$nm, respectively. A three dimensional finite element model is also established to obtain the SWNT temperature. The good agreement between the analytical prediction and finite element simulations validates the analytical model. The temperature rise of SWNT rapidly increases to maximum at the end of pulse duration (i.e., $t = t_d$) and then drops to nearly zero during the rest in one period. For example, the temperature rise decreases to $\sim 10^{-4}\%$ of its maximum after 10 ns cooling and $\sim 10^{-9}\%$ at the end of the period 1 ms. These results suggest that the SWNT completely cool to the ambient temperature between pulses without appreciable cumulative heating.

Figure 4 shows the maximum normalized temperature rise $\bar{\theta}_{SWNT}^{Max} = \rho c \alpha \sigma^2 \theta_{SWNT}^{Max}/[(1 - e^{-\delta d})P_0 R]$ versus the normalized laser pulse duration $\bar{t}_d = t_d \alpha/R^2$ at different normalized interfacial thermal resistance $\bar{R}_{th} = R_{th}\rho c \alpha/R$. Here, we take $\bar{R}_{th} = 0$, 60, and 600 corresponding to $R_{th} = 0$, $10^{-8}$, and $10^{-7}$ m$^2$K/W, respectively. The finite element results for $\bar{t}_d = 0.273$ and $2.73 \times 10^4$ corresponding to $t_d = 100$fs and 10 ns, and the approximate solution for a small $\bar{t}_d$ are also shown for comparison. It is shown that the analytical predictions agree well with finite element simulations at both small $\bar{t}_d$ and large $\bar{t}_d$. Equation (9) gives a good approximation at a small $\bar{t}_d$. The maximum normalized temperature rise $\bar{\theta}_{SWNT}^{Max}$ first increases linearly as the normalized pulse
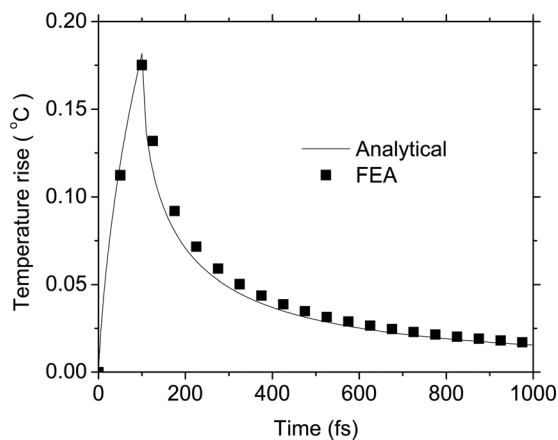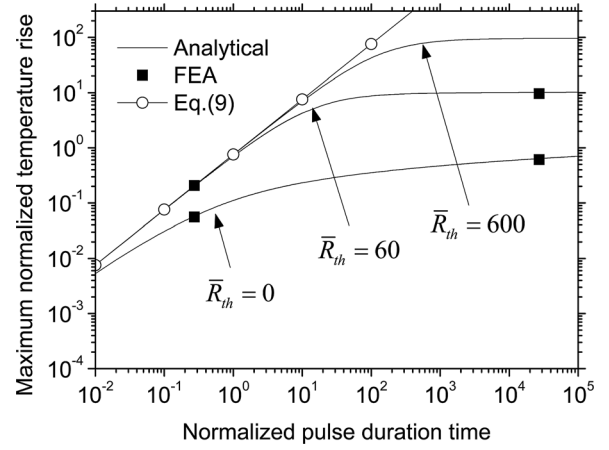


FIG. 4. The maximum normalized temperature rise $\bar{\theta}_{SWNT}^{Max} = \rho c \alpha \sigma^2 \theta_{SWNT}^{Max}/[(1 - e^{-\delta d})P_0 R]$ versus the normalized laser pulse duration $\bar{t}_d = t_d \alpha/R^2$ at different normalized interfacial thermal resistance $\bar{R}_{th} = R_{th}\rho c \alpha/R$.

duration time $\bar{t}_d$ increases and then reaches the steady solution. The existence of interfacial thermal resistance increases the normalized temperature rise. For a realistic $\bar{R}_{th}$ ranging from 60 to 600, $\bar{R}_{th}$ increases $\bar{\theta}_{SWNT}^{Max}$ at a large $\bar{t}_d$, while it has a negligible effect at a small $\bar{t}_d$. The reason is that when $\bar{t}_d$ is small, most of the energy is used to heat s-SWNT itself and the energy passing through the interface is negligible, which is to be further illustrated in Fig. 5.

Figure 5 shows the fraction of energy $\gamma$ into the substrate versus the normalized laser pulse duration $\bar{t}_d = t_d \alpha/R^2$ at different normalized interfacial thermal resistance $\bar{R}_{th} = R_{th}\rho c \alpha/R$. It clearly shows that at a small $\bar{t}_d$, $\gamma$ is nearly zero, i.e., most of the energy is used to heat the m-SWNT, while at a large $\bar{t}_d$, $\gamma$ is nearly 1, i.e., the self-heating of m-SWNT is negligible and most of the energy passes through the interface to heat the substrate.

## V. CONCLUSIONS

In summary, we have established a scaling law, validated by finite element simulations, for the SWNT
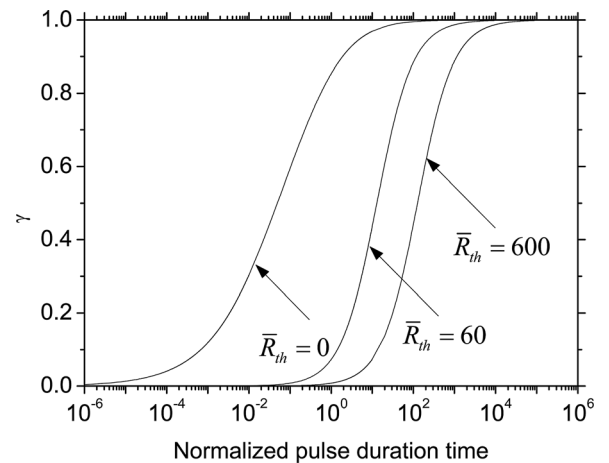


FIG. 3. The temperature rise of the m-SWNT at $x = 0$ as a function of time with $t_d = 100$fs, $t_p = 1$ms, $P_0 = 1.0$W, $\sigma = 0.6\mu m$, $R_{th} = 0$, and $1 - e^{-\delta d} = 0.068$.



FIG. 5. The fraction of energy $\gamma$ into the substrate versus the normalized laser pulse duration $\bar{t}_d = t_d \alpha/R^2$ at different normalized interfacial thermal resistance $\bar{R}_{th} = R_{th}\rho c \alpha/R$.

temperature rise under a pulsed laser with a Gaussian spot. The maximum normalized SWNT temperature rise only depends on the normalized pulse duration time and the normalized interfacial thermal resistance. It is shown that self-heating of the SWNT is dominant for a small pulse duration time while it is negligible for a large pulse duration time. In addition, the maximum temperature rise is inversely proportional to the square of spot size and proportional to the incident laser power. The above results may serve as design guidelines for system optimization especially for determining the optimal condition to remove the m-SWNTs.

[1]P. Avouris, Z. Chen, and V. Perebeinos, Nat. Nanotechnol. **2**, 605 (2007).

[2]S. J. Kang, C. Kocabas, T. Ozel, M. Shim, N. Pimparkar, M. A. Alam, S. V. Rotkin, and J. A. Rogers, Nat. Nanotechnol. **2**, 230 (2007).

[3]C. Wang, K. Takei, T. Takahashi, and A. Javey, Chem. Soc. Rev. **42**, 2592 (2013).

[4]M. A. Alam, N. Pimparkar, S. Kumar, and J. Murthy, MRS Bull. **31**, 466 (2006).

[5]L. Hu, D. S. Hecht, and G. Gruner, Nano Lett. **4**, 2513 (2004).

[6]P. N. Nirmalraj, P. E. Lyons, S. De, J. N. Coleman, and J. J. Boland, Nano Lett. **9**, 3890 (2009).

[7]J. Xiao, S. Dunham, P. Liu, Y. Zhang, C. Kocabas, L. Moh, Y. Huang, K. C. Hwang, C. Liu, W. Huang, and J. A. Rogers, Nano Lett. **9**, 4311 (2009).

[8]S. H. Jin, S. N. Dunham, J. Song, X. Xie, J. H. Kim, C. Lu, A. Islam, F. Du, J. Kim, J. Felts, Y. Li, F. Xiong, M. A. Wahab, M. Menon, E. Cho, K. L. Grosse, D. J. Lee, H. U. Chung, E. Pop, M. A. Alam, W. P. King, Y. Huang, and J. A. Rogers, Nat. Nanotechnol. **8**, 347 (2013).

[9]P. C. Collins, M. S. Arnold, and P. Avouris, Science **292**, 706 (2001).

[10]M. M. Shulaker, G. Hills, N. Patil, H. Wei, H. Y. Chen, H. S. P. Wong, and S. Mitra, Nature **501**, 526 (2013).

[11]X. Xie, S. H. Jin, M. A. Wahab, A. E. Islam, C. Zhang, F. Du, E. Seabron, T. Lu, S. N. Dunham, H. I. Cheong, Y. C. Tu, Z. Guo, H. U. Chung, Y. Li, Y. Liu, H. H. Lee, J. Song, Y. Huang, M. A. Alam, W. L. Wilson, and J. A. Rogers, Nat. Commun. **5**, 5332 (2014).

[12]F. Du, J. R. Felts, X. Xie, J. Song, Y. Li, M. R. Rosenberger, A. E. Islam, S. H. Jin, S. N. Dunham, C. Zhang, W. L. Wilson, Y. Huang, W. P. King, and J. A. Rogers, ACS Nano **8**, 12641 (2014).

[13]J. Song, C. Lu, C. Zhang, S. H. Jin, Y. Li, S. N. Dunham, X. Xie, F. Du, Y. Huang, and J. A. Rogers, RSC Adv. **4**, 42454 (2014).

[14]S. H. Jin, J. Song, H. U. Chung, C. Zhang, S. N. Dunham, X. Xie, F. Du, T. Kim, J. H. Lee, Y. Huang, and J. A. Rogers, J. Appl. Phys. **115**, 054315 (2014).

[15]M. Mahjouri-Samani, Y. S. Zhou, W. Xiong, Y. Gao, M. Mitchell, and Y. F. Lu, Nanotechnology **20**, 495202 (2009).

[16]X. Bai, D. Li, D. Du, H. Zhang, L. Chen, and J. Liang, Carbon **42**, 2125 (2004).

[17]M. Yudasaka, M. Zhang, and S. Iijima, Chem. Phys. Lett. **374**, 132 (2003).

[18]P. Nikolaev, O. Gorelik, R. Allada, E. Sosa, S. Arepalli, and L. Yowell, J. Phys. Chem. C **111**, 17678 (2007).

[19]H. Huang, R. Maruyama, K. Noda, H. Kajiura, and K. Kadono, J. Phys. Chem. B **110**, 7316 (2006).

[20]B. Zandian, R. Kumar, J. Theiss, A. Bushmaker, and S. B. Cronin, Carbon **47**, 1292 (2009).

[21]A. Roch, T. Roch, E. R. Talens, B. Kaiser, A. Lasagni, E. Beyer, O. Jost, G. Cuniberti, and A. Leson, Diamond Relat. Mater. **45**, 70 (2014).

[22]P. A. Danilov, A. A. Lonin, S. I. Kudryashov, S. V. Makarov, N. N. Mel'nik, A. A. Rudenko, V. I. Yurovskikh, D. V. Zayarny, V. N. Lednev, E. D. Obraztsova, S. M. Pershin, and A. F. Bunkin, Laser Phys. Lett. **11**, 106101 (2014).

[23]S. Ferrari, M. Bini, D. Capsoni, P. Galinetto, M. S. Grandi, U. Criebner, G. Steinmeyer, A. Agnesi, F. Pirzio, E. Ugolotti, G. Reali, and V. Massarotti, Adv. Funct. Mater. **22**, 4369 (2012).

[24]M. Ichida, S. Saito, T. Nakano, Y. Feng, Y. Miyata, K. Yanagi, H. Kataura, and H. Ando, Solid State Commun. **151**, 1696 (2011).

[25]E. Pop, D. A. Mann, K. E. Goodson, and H. Dai, J. Appl. Phys. **101**, 093710 (2007).

[26]F. Xiong, A. Liao, and E. Pop, Appl. Phys. Lett. **95**, 243103 (2009).

[27]A. Liao, R. Alizadegan, Z. Y. Ong, S. Dutta, F. Xiong, K. J. Hsia, and E. Pop, Phys. Rev. B **82**, 205406 (2010).

[28]H. S. Carslaw and J. C. Jaeger, *Conduction of Heat in Solids*, 2nd ed. (Clarendon Press, Oxford, 1959), p. 510.

[29]R. B. Pipes, S. J. V. Frankland, P. Hubert, and E. Saether, Compos. Sci. Technol. **63**, 1349 (2003).

[30]J. P. Lu, Phys. Rev. Lett. **79**, 1297 (1997).

[31]C. Y. Li and T. W. Chou, Int. J. Solids Struct. **40**, 2487 (2003).

[32]D. G. Cahill, W. K. Ford, K. E. Goodson, G. D. Mahan, A. Majumdar, H. J. Maris, R. Merlin, and S. R. Phillpot, J. Appl. Phys. **93**, 793 (2003).

[33]H. K. Lyeo and D. G. Cahill, Phys. Rev. B **73**, 144301 (2006).